

Advances in MgB₂ Superconductor Applications for Particle Accelerators

Akira Yamamoto^{1,2} 

¹ High Energy Accelerator Research Organization (KEK), Tsukuba, Japan

² European Organization of Nuclear Research (CERN), Geneva, Switzerland

E-mail: akira.yamamoto@kek.jp

arXiv: 2201/09501, submitted: Jan. 24, 2022, and to be updated, Feb. 11, 2022.

Abstract

The MgB₂ superconductor, discovered in 2001, has provided unique compound features of magnesium diboride with much higher critical temperature and critical field compared to NbTi superconductor. Its applications have been expanding owing to its superior energy balance in high-temperature operation and to its excellent stability and operational margin because of the higher critical temperature and heat capacity. This paper reviews the recent advances in MgB₂ applications in the field of particle accelerators focusing on superconducting power transmission (superconducting link) and superconducting magnets, and also briefly discusses the future prospects and improvement expected such as radiation hardness issues and cost-effective fabrication for wider applications and industrialization.

Keywords: MgB₂, Magnesium-Diboride superconductor, Superconducting magnets, Superconducting link, Particle accelerators.

1. Introduction

Since the discovery of the MgB₂ superconductor in 2001¹⁾, superconductor development and applications have advanced significantly owing to various research institute efforts²⁻⁶⁾. Three leading companies have pursued industrial effort: ASG (formally known as Columbus), HyperTech, and Hitachi⁷⁻¹³⁾. ASG has led the development of high-current conductors by using ex situ methods, while HyperTech has been leading the development of using in situ methods characterized by filament thinning and AC applications. As for Hitachi, they focus on the development of the ‘modified in situ’ methods, which results in the superconductors featured in high current density and magnetic field applications. **Figure 1** shows a comparison of the typical MgB₂ engineering critical current densities as a function of the external magnetic field reported by the three companies.

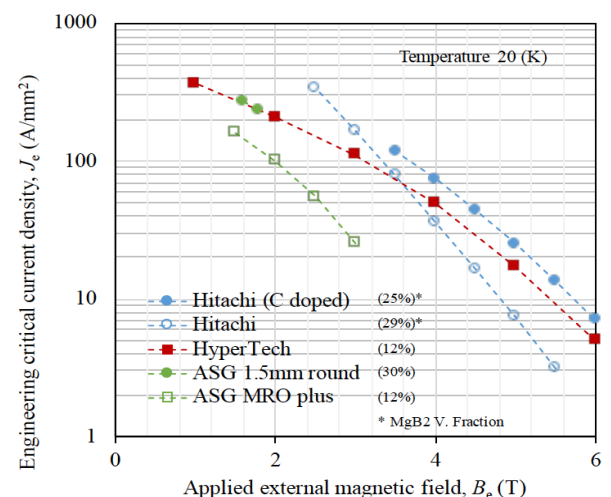


Fig. 1. Typical Engineering current densities (J_e) as a function of magnetic field (B_e) for MgB₂ wires/strands commercially available from ASG, HyperTech, and Hitachi^{7, 8, 12)}.

This report presents the recent progress in the application of MgB₂ superconductors, particularly in the field of particle accelerators and associated devices. These applications utilize the significantly higher critical temperature to provides stability. The future prospects of this technology are also briefly discussed.

This review article, in English, has been translated and summarized from the originally articulated published in ‘TEION KOGAKU’ 57 (2022), in Japanese¹⁴.

2. Advances in MgB₂ Superconductor Applications

2.1 Superconducting Link for the HL-LHC IR magnets

The High-Luminosity Large Hadron Collider (HL-LHC) project has been under construction at the European Organization for Nuclear Research (CERN) since 2018¹⁵. One of its requirements is the isolation of radiation-sensitive power supplies and associated control systems from superconducting magnets placed in the high-radiation area of the accelerator tunnel (e.g., the beam interaction regions (IRs)). These are necessary to eliminate operational errors in the power supplies and control system owing to phenomena such as high neutron irradiation. Therefore, the magnet power supply systems must be in a separate tunnel at a distance at least 100 m, and the power is transmitted by the superconducting link (see Fig. 2)¹⁵.

A MgB₂ superconducting cable has been implemented to a superconducting link with a set of 100 kA power-supply currents¹⁶⁻¹⁸. The main parameters of the single MgB₂ superconducting wire are listed in Table 1. A total of 21 circuits with a total capacity of 150 kA are assembled and integrated into a cable complex with a diameter of 90 mm, (see

Table 1. MgB₂ wire specification for the CERN HL-LHC superconducting link, manufactured by ASG¹⁸

Wire diameter	1 mm
Cu fraction	≥ 12 %
Filament eq. diameter	≤ 60 μm
Filament twist pitch	100 mm
Tensile strain at RT (w/o I _c degradation)	≥ 0.26%
Bending radius after heat treatment	≤ 100 mm
RRR (Cu)	≥ 100
I _c (@ 25 K, 0.5 Tesla)	≥ 320 A
(@ 20 K, 0.5 Tesla)	≥ 480 A

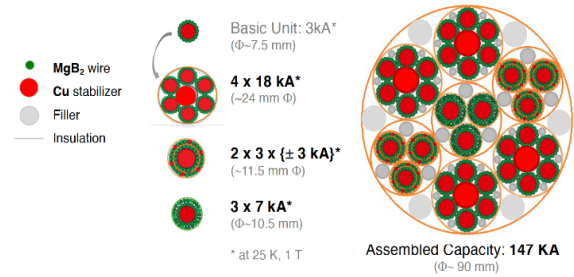


Fig. 3. Superconducting cable assembly¹⁸.

Fig. 3). The setup is as follows: four 18 kA cables for the IR final focusing quadrupole magnets (Q1-Q3) and the beam separation dipole magnets (D1), three 7 kA cables for the Q1-Q3 current trimming, and three pairs of 3 kA cables for the correction/steering magnets. Finally, the cross sections of the wires and cables are integrated into 21 circuits.

This cable is assembled into a flexible bellows-shaped cryostat (i.e., a flexible transfer tube) along with a flexible adiabatic vacuum piping whose outer diameter was 300 mm,

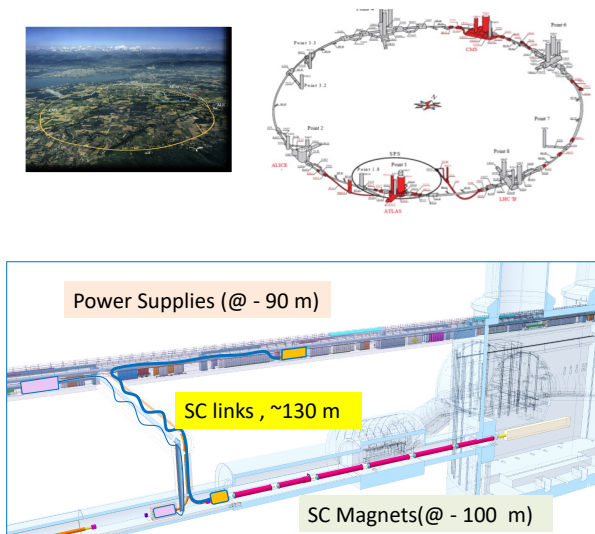
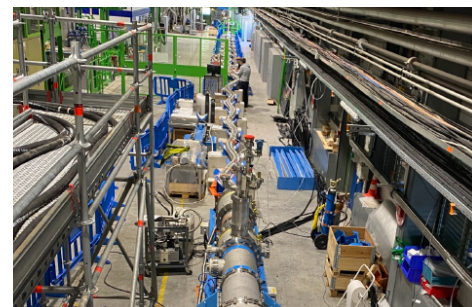


Fig. 2. Superconducting power transmission (SC links) with a current capacity of 150 kA and with a length of 100 m for the CERN HL-LHC superconducting magnet beam line¹⁵.

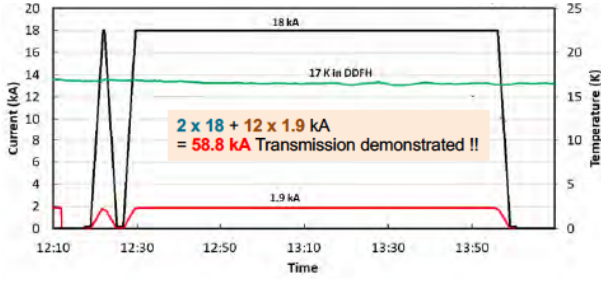


(a)



(b)

Fig. 4. SC link prototype setup at a test facility in 2020¹⁸.



(b)

Fig. 5. Superconducting link prototype layout, and (b) successfully demonstrated up to 58.8 kA transmission in a flexible 60 m cryostat at a test station in 2020¹⁸⁾.

which also functioned as a flexible liquid helium transfer line. A high-temperature superconductor transition is placed at the power supply end, and a gas-cooled current lead is placed at the extraction end to ensure a room-temperature connection. A prototype of the MgB₂ superconducting link technology has been successfully developed (see Fig. 4) and has shown promising results. The results of the power transmission test, which has been performed in a test facility, are shown in Fig. 5¹⁸⁾. This prototype MgB₂ superconducting link test has shown extremely stable superconducting power transmission while maintaining a high critical temperature and significantly larger specific heat at 25 K. The production of the superconducting cables is in progress, and the superconducting link operation is to be realized in later 2020s. In the future, owing to their high energy efficiency and improved safety, wider applications such and high-power transmission in a grid network can be expected¹⁸⁾.

2.2 Superconducting solenoids for High-efficiency RF power supplies of CLIC.

The Compact Linear Collider (CLIC) has been proposed as a future candidate for an electron-positron collider accelerator at CERN¹⁹⁾. The plan is first to build a collider that can reach a center-of-mass energy of 380 GeV (i.e., CLIC-380), and then upgrade it to reach 3 TeV in the future. The CLIC uses a two-beam acceleration scheme, wherein a normal-conducting high-gradient 12 GHz accelerating structures are powered via a high-current drive beam. In the first stage (CLIC-380), an alternative to X-band klystron powering is also considered, as illustrated in Fig. 6. A klystron, consisting of a small electron-beam accelerator for radio-frequency (RF) power amplification in the klystron requires beam focusing with a solenoidal magnetic field of 0.6 to 0.7 T²⁰⁾. A conventional copper solenoid magnet, as shown in Fig. 7 (a), consumes an AC plug power of 20 kW, resulting in 100 MW consumption with 5,000 klystrons. The application of MgB₂ superconducting solenoid magnets at an operational temperature of 20 K may contribute to power savings of an

order of magnitude²¹⁾. This is because it only requires cryogenic operation power. A prototype MgB₂ superconducting solenoid magnet (see Fig. 7(b)) was developed and conductively cooled using a cryocooler whose

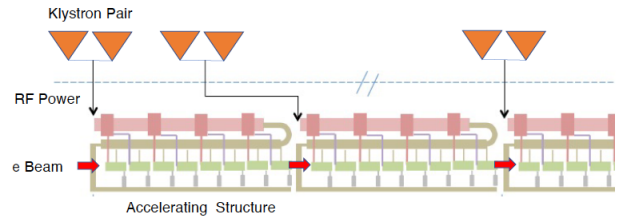


Fig. 6. The CLIC-380 concept with klystrons supplying RF power to normal conducting accelerator structure¹⁸⁾.

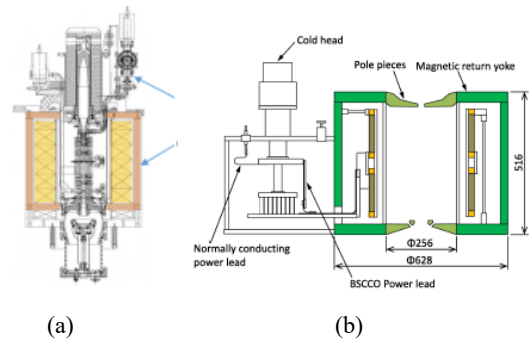


Fig. 7. 12 GHz Klystron assembled with conventional (Cu) solenoid, and (b) MgB₂ solenoid prototype replacing the Cu solenoid²⁰⁻²²⁾.

Table 2. Parameters of the MgB₂ prototype solenoid²¹⁾.

MgB ₂ : Conductor configuration	MgB ₂ /Cu/Fe/Monel
Strand diameter	0.67 mm
Coil: Inner diameter, length	0.34, 0.3 m
Current	57 A
Central field	0.8 T
Stored energy	11.8 kJ
Cryostat: ID, OD	0.25, 0.63
Cooling capacity	4 W at 20 K
AC plug power	2.8 kW at 300 K

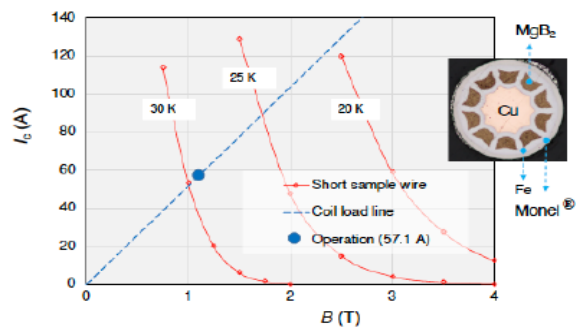


Fig. 8. MgB₂ superconductor operational characteristics^{13, 21)}.

main parameters and load line characteristics are shown in **Table 2** and **Fig. 8**, respectively^{21, 22}). Stable operation at a temperature range of 20–25 K was confirmed with an AC plug power of < 3 kW for cryocooler operation, resulting in almost one order of magnitude of power saving compared with the normal-conducting copper solenoid. If extended to large-scale applications (i.e., CLIC-380), it can save 100 MW of power for 5,000 klystrons. Based on this, if the operational temperature is relatively high (i.e., 60 - 70 K), HTS applications can expect additional power savings²¹). However, this is under the assumption that cost-effective HTS is accessible.

2.3 Superconducting magnets for the main linac of ILC

The International Linear Collider (ILC) is a proposed energy frontier electron-positron collider with the Technical Design Report published in 2013²³). This includes a stepwise upgrade plan to reach a center-of-mass energy of 500 GeV to 1 TeV. In 2017, the design was updated to the beginning of the first phase with a center-of-mass energy of 250 GeV with a total length of 20.5 km, known as the Higgs factory²⁴). **Figure 9** shows the ILC main linac composed of superconducting radio frequency (SRF) cavity and superconducting (SC) magnet strings in a series of cryomodules. The ILC linearly accelerates electrons and positrons, facing each other by using the series of SRF cavities that realizes e^+e^- head-on collisions at the central region of the accelerator complex. The SC magnets are required for beam focusing and orbit control/steering, combined with the beam acceleration by the SRF cavities installed in the cryomodule as shown in **Figs. 10 (a), (b), and (c)**. These magnets are installed at intervals of 40 m in a series of SRF cavity strings. The magnet parameters are summarized in **Table 3**^{25, 26}). A super-ferric SC magnet design with conduction cooling has been chosen to enable the magnet structure to be split to assemble the magnet surrounding the beam pipe after the SRF cavity string and beam pipe assembly finished in a clean room. The SC magnet is conductively cooled with no liquid helium vessel available because of the splittable structure²⁷

A technical issue with the ILC main-linac superconducting magnet is coil heating caused by the energy absorption of the field-emitted electron flow (i.e., dark current) initiated by a very high electric field on the inner surface of the SRF cavities located upstream, as illustrated in **Fig. 11**²⁸⁻³⁰). The dark-current electrons are accelerated by the electric field in the

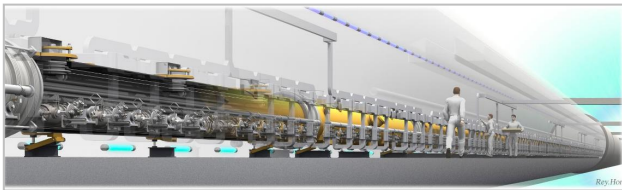


Fig. 9. ILC main linac with SRF cavity strings and magnets²³).

SRF cavity and then transferred to the superconducting magnet location. The dark current electrons with relatively low energy are largely deflected by the magnetic field, and the energy is absorbed by the superconducting magnet. The temperature increase in the coil due to energy absorption causes the risk of the NbTi superconductor to exceed its current-sharing critical temperature. Thus, MgB₂/Nb₃Sn superconductors may significantly reduce this risk, as summarized in **Table 4**. The Superconductor and the magnet load-line characteristics focusing on the critical temperatures for NbTi, N₃Sn and MgB₂ at an expected operational current of 100 A at 3 T are shown in **Fig. 12**.

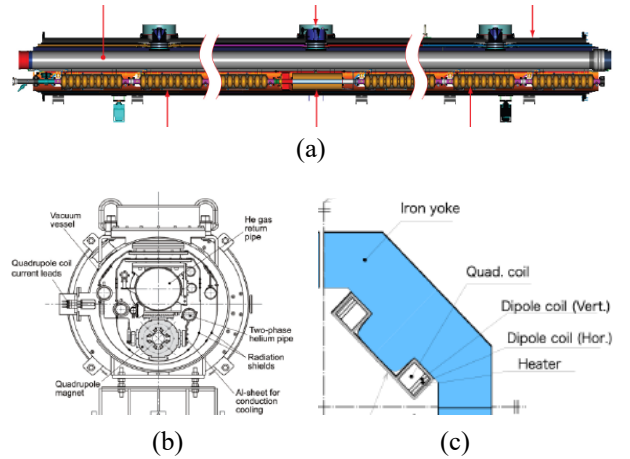


Fig. 10. (a) ILC main linac cryomodule (side view) consisting of a SRF cavity string with superconducting (SC) magnet placed at center, (b) cross-section of the cryomodule with the SC magnet, and (c) the cross-section of the SC magnet composed of quadrupole and dipole coils and iron yoke^{23, 25, 26}).

Table 3. Main parameters of the ILC-ML SC combined function magnet for the ILC main linac²⁶).

Items	Parameters
Physical, magnetic length	1 m, 0.95 m
Inner aperture radius	0,045 m
Quadrupole Field gradient (G)	40 T/m
Dipole Corrector field (B)	0.11 T
Peak magnetic field in Coil (B _p)	3 T
Operational Temperature (T _o)	2 K

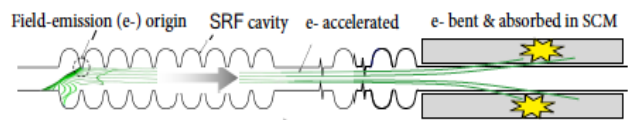


Fig. 11. Dark current electrons accelerated by SRF cavity string²⁸⁻³⁰).

Table 4. Characteristics of NbTi, Nb₃Sn, and MgB₂ wires for ILC-ML SC magnet under dark current absorption^{26,30)}.

Item	unit	NbTi	Nb ₃ Sn	MgB ₂
Strand diameter	mm	0.5	0.6	0.55
Cu / SC ratio		2	1	0.8
I _{op} at 3 T	A	100	100	100
T _c at 3 T, 100 A	K	7	13	15
C _p at T _c	kJ/kg/K	~ 0.3	~ 2	~ 2.5
dh to T _c at 3 T	J/kg	~ 0.8	~ 6	~ 8

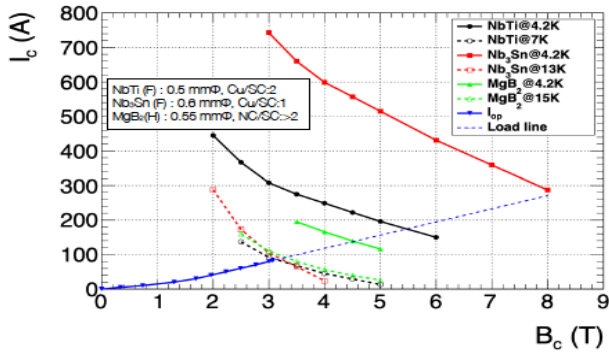


Fig. 12. Critical current (I_c) as a function of critical field (B_c) for NbTi, Nb₃Sn, and MgB₂, and a load-line of the ILC main-linac magnet package^{26, 30)}.

2.4. Superconducting magnets for J-PARC stretcher ring

The Japan Proton Accelerator Research Complex (J-PARC), jointly established by JAEA and KEK, is a multifunctional accelerator complex that provides various quantum beams (e.g., hadrons, neutrinos, K mesons, muons, and neutrons) for particle and nuclear physics as well as materials and life sciences³¹⁾. The J-PARC main-ring (MR) proton synchrotron supplies neutrino beams for the long-baseline neutrino oscillation experiment (T2K: Tokai-to-Kamioka) using a fast-extracted proton beam. Furthermore, it also supplies hadron and meson beams for the hadron and meson physics using a smoothed slow-extracted beam. It is anticipated that both fast and slow-extracted beams are realized in parallel. A stretcher ring is proposed to be added above the existing MR synchrotron in the same tunnel (see **Figs. 13(a)** and **(b)**)³²⁾. The objective here is the power-efficient enhancement of the overall beam intensity, based on DC-mode operation, using superconducting magnets for storing and slowly extracting the proton beam for hadron/meson experiments. MgB₂ is a viable option for stretcher ring magnets to improve the AC plug power efficiency because it can operate at relatively higher temperatures. A combined-function, super-ferric magnet design was investigated (see **Fig. 13(c)** for the conceptual cross-section), for the generation of a dipole field of 1.15 T

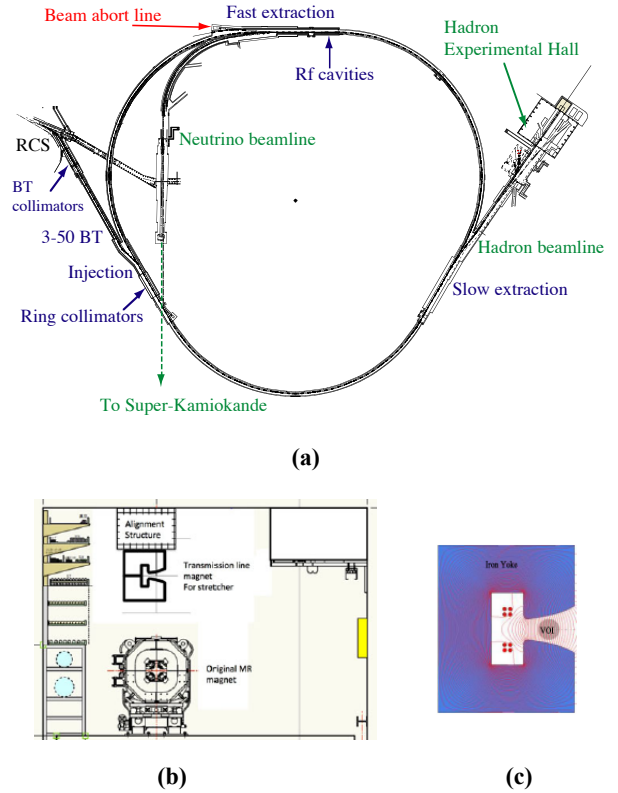


Fig. 13. (a) Layout of J-PARC Main Ring and (b) the accelerator tunnel cross section with the current MR magnets (bottom) and (c) a possible stretcher-ring magnet X-section using MgB₂ superconducting cable technology^{32, 33)}.

and a quadrupole field gradient of 40 T/m³³⁾. The MgB₂ power transmission cable, as discussed for the HL-LHC superconducting link¹⁸⁾, is an interesting option for simplifying magnet design using the concept of ‘transmission line’. Cost-effective magnet design can be achieved using this approach.

2.5. Medical accelerator Applications

MgB₂ applications in heavy-ion synchrotron accelerators for cancer therapy may be considered, as it would reduce the size of the accelerator complex and gantry beamlines and operational costs^{34, 35)}. Size reduction is of particular interest and important as it allows for variable-angle beam irradiation. By adopting MgB₂, an operating temperature range of < 25 K and a magnetic field strength of < 3 T can be expected and the operational cost may be significantly reduced for wider applications.

3. Summary and Prospect

MgB₂ superconductor applications have advanced in the field of particle accelerators and their associated devices. These applications are characterized by the necessity of an

optimum magnetic field in the range of < 3 T, high specific heat, and an operating temperature of 20 K. These properties are necessary to ensure device stability. Furthermore, when combined with liquid hydrogen cooling, the resulting device will also be significantly more energy-efficient than existing systems. However, it should be noted that there are very important issues that need to be addressed before their practical use in particle accelerators. For example, the radiation resistance of the material remains unexplored and is of great concern because the neutron-boron interaction cross-section is known to be relatively large. Furthermore, the capable current stability and sustainability still needs to be verified. Lastly, the cost reduction of the MgB₂ composite fabrication technology is very important for it to be of interest in wider applications.

Acknowledgements

The author would like to thank Dr. Kumakura (NIMS), Mr. G. Grasso (ASG), Mr. M. Rindfleisch (HyperTech), and Dr. H. Tanaka (Hitachi) for providing information on the development of MgB₂ superconductors. He would sincerely thank Dr. A. Ballarino (CERN) for providing the MgB₂ superconducting link application information for the HL-LHC and various discussions. He would thank Prof. T. Koseki and Prof. T. Ogitsu (KEK) for providing the J-PARC stretcher ring feasibility study for the future update. The MgB₂ solenoid frbrlopnrnyy for the high-efficiency klystrons has been realized with the CERN-KEK-Hitachi cooperation oversighted by Dr. S. Stapnes (CERN).

The author is sincerely indebted to Cryogenics and Superconductivity Society of Japan (CSSJ), publishing ‘TEION KOGAKU’ for the kind permission for the original review published in Japanese to be translated to English and to be published in a journal widely distributed in this field.

The authors would express sincere thanks to Editage (www.editage.com) for English language editing.

ORCID iD

Akira Yamamoto  <https://orcid.org/0000-0002-5917-3411>

References

- [1] J. Nagamatsu, A.J. Kimitsu *et al*: *Nature* **410** (2001) 63–64.
- [2] G. Giunchi *et al*: *Supercond. Sci. Technol.* **16** (2003) 285–291.
- [3] S. Ye *et al*: *Supercond. Sci. Technol.* **29** (2016) 11304.
- [4] H. Kumakura *et al*: *TEION KOGAKU* **56** (2021) 317–326.
- [5] H. Kumakura Abstract of CSJ Conference **101** (2021) 50 .
- [6] M. Sumption *et al*: *AIAA Propulsion & Energy Forum* (2019) 10.2514/6.2019-4495.
- [7] G. Grasso: *ASC Superconductor* (2021-11-27), URL available, <https://www.asgsuperconductors.com/>
- [8] T.A. Prikhna, Eisterer M, Rindfleisch M *et al*: *IEEE Trans. Appl. Supercond.* **29** (2019) 6200905.
- [9] T. Baig *et al*: *Supercond. Sci. Technol.* **30** (2017) 043002
- [10] I. Bejar, P. Fessia, L. Rossi, O. Bruning *et al* (eds): *CERN-I* 2017-007-M (2017).
- [11] H. Tanaka *et al*: *IEEE Trans. Appl. Supercond.* **27** (2017) 4600904.
- [12] H. Tanaka *et al*: *IEEE Trans. Appl. Supercond.* **30** (2020) 6200105.
- [13] H. Tanaka and M. Kodama: *TEIONKOGAKU* **56** (2021) 327–334 (in Japanese).
- [14] A. Yamamoto: *TEIONKOGAKU* **57** No. 1 (2022) 17–22 (in Japanese).
- [15] I. Alonso *et al*: CERN Yellow Reports, CERN-2017-004 (2017), <https://doi.org/10.23731/CYRM-2017-004>.
- [16] A. Ballarino *et al*: *Supercond. Sci. Technol.* **27** (2014) 044024.
- [17] A. Ballarino *et al*: *IEEE Trans. Appl. Supercond.* **26** (2016) 5401705.
- [18] A. Ballarino: *Int. Particle Acc. Conf. IPAC’21* (2021), and announced by CERN news, <https://home.cern/news/news/accelerators/electricity-transmission-reaches-even-higher-intensities>
- [19] M. Aicheler *et al*: *CERN Yellow Reports*, CERN-2018-010-M20 (2018), <https://doi.org/10.23731/CYRM-2018-004>
- [20] F. Peauger *et al*: *Proc. IPAC’10* (2010).
- [21] A. Yamamoto *et al*: *IEEE Trans. Appl. Supercond.* **30**, (2020) 4101304.
- [22] H. Watanabe *et al*: *IEEE Trans. Appl. Supercond.* **30** (2020) 4601206.
- [23] A. Abada *et al*: *KEK Report, KEK 2013-1* (2013), <https://inspirehep.net/literature/1240418>
- [24] P. Bambade *et al*: *ESPPU’20* (2019-3-5); arXiv:1903.01629v3 [hep-ex], updated 5 Apr 2019.
- [25] V.S. Kashikhin *et al*: *IEEE Trans. Appl. Supercond.* **22** (2012) 4002904.
- [26] Y. Arimoto *et al*: *Proc. IPAC’21* (2021) TUPAB017.
- [27] H. Shimizu *et al*: to be published in *IEEE Trans. Appl. Supercond.* (2022).
- [28] Y. Li, K. Liu, R. Geng, and A. Palczewski: *Proc. SRF2013* (2013) TUIOA06.
- [29] A. Sukhanov, I. Rankhno, N. Solyak *et al*: *Proc. LINAC2016* (2016) THPLR007.
- [30] A. Yamamoto and N. Solyak: TESLA Technology Collaboration meeting (2021). <https://indico.desy.de/event/27572/timetable/#20210120.detail> ed
- [31] J-PARC URL: <https://j-parc.jp/c/en/index.html>
- [32] M. Tomizawa *et al*: *IPAC’18* (2018) TUPML055, and *IOP Conf. Series: Journal of Physics* **1067** (2018) 042004.
- [33] T. Ogitsu *et al*: *IEEE Trans. Appl. Supercond.* **27** (2017) 4003705.
- [34] Y. Hirao *et al*: *NIRS-M-89* (1992) .
- [35] H. Souda *et al*: *Kasokuki*, **17** (2020) 1140150.